Hindawi
Mathematical Problems in Engineering
Volume 2019, Article ID 1269064, 10 pages
https://doi.org/10.1155/2019/1269064

Research Article

Influence Zone Division and Risk Assessment of Underwater Tunnel Adjacent Constructions

Zhong Zhou, Wenyuan Gao, Zhuangzhuang Liu, and Chengcheng Zhang

School of Civil Engineering, Central South University, Changsha 410075, China

Correspondence should be addressed to Zhong Zhou; 369144091@qq.com

Received 25 August 2018; Revised 20 November 2018; Accepted 24 December 2018; Published 15 January 2019

Guest Editor: Gerhard-Wilhelm Weber

Compared with ordinary tunnels, the influence analysis of underwater tunnel adjacent constructions is more complicated. At present, the empirical method used to divide the influence zone of the tunnel adjacent constructions has great uncertainty. So it is of great significance for actual construction and design to determine the influence zone accurately according to theoretical calculations. In this paper, based on the Hoek–Brown nonlinear failure criterion of rock mass and taking seepage factor into account, the stress state of rock mass around the underwater tunnel adjacent constructions can be deduced by elastoplastic theory. Then combined with the concept of "loose zone-bearing zone", the influence zone division method of underwater tunnel adjacent constructions is proposed, and it is applied to the analysis of engineering examples. Through the deduced theoretical formulas, the influence zone of underwater tunnel adjacent construction can be divided into extensively strong, strong, relatively strong, weak, and noninfluence zones. Corresponding the influence zones with the risk levels in the code, different control measures are adopted for different risk levels, which can provide certain guidance for the design and construction of tunnel in practical engineering.

1. Introduction

Presently, the development of urban subway traffic construction is rapid. As the utilization ratio of land resources and building space in the city is gradually improved, tunnel construction inevitably will be close to existing structures, which makes tunnel adjacent construction become the key link in current tunnel design and construction, and underwater tunnel is no exception. However, due to its more difficult construction, more complicated conditions, and more stringent requirements, the underwater tunnel adjacent construction is different from ordinary tunnels. How to evaluate the impact of underwater tunnel construction on adjacent structures is of great guiding significance for tunnel line selection and site construction.

The local and overseas scholars have performed outstanding achievement regarding the influence zone division of tunnel adjacent constructions. In 1998, Japan made a guideline for the construction of railway, highway, and electric power industries which lead to the beginning of the study on the influence zone of adjacent construction [1]. In recent years, the research on the theory of zoning has been further developed. In terms of experimental research, the team of Chou [2] systematically summarized the local cases of recent construction projects, studied the impact of adjacent construction, and proposed the zoning method of different types of adjacent construction. For example, when two tunnels are parallel (where L is the distance between the two tunnels), L <1D is the strong influence area, and 1D≤L <2.5D is the weak influence area. Thereafter, most of the studies are similar. Du [3] relied on the tunnel in Shanghai to carry out in situ tests of soil disturbance. Based on the soil disturbance data, the degree of influence was divided. Li et al. [4] deduced the disturbed plastic zone of soil under tunnel construction based on hole expansion theory. The plastic zone was regarded to strong influence zone, and the field test and the finite element method were used to verify this finding. Other scholars conducted further research on the basis of different engineering test data. In terms of numerical simulation, Huang et al. [5] used a series of centrifuge model tests conducted to investigate the effect of deep excavation above an existing tunnel. Xu et al. [6] studied the influence shield tunneling on surround soils through the monitoring in situ and analyzed the soil disturbance by variation of the

stress due to shield tunneling. Tao et al. [7] calculated the stress of infinite elastic plate by using elastic theory of plane strain, in which the stress and the different stress of it only caused before metro tunnel excavation were piled up, and then derived ground settlement curve equation from the solution of infinite elastic plate. Huang et al. [8] presented a finite-element parametric study of tunnel behavior caused by nearby deep excavation and investigated the effects of several parameters that may affect the tunnel response. Wang et al. [9] established a three-dimensional simulation method that can fully reflect the whole process of shield tunneling to study the impact of the adjacent construction to the pile foundation. Liu et al. [10] investigated the effects of pipe jacking on existing underlying tunnels and analyzed the vertical displacement, horizontal displacement, and diameter convergence of the tunnel based on the field observations. Avgerinos et al. [11] developed a basic three-dimensional (3D) finite-element (FE) model and discussed changes in hoop forces, bending moments, and lining deformations of the exiting tunnel due to excavation of the new tunnel. Zhang et al. [12] presented the deformation analyses of existing subway tunnels induced by an earth pressure balance (EPB) shield during the process of above-overlapped and down-overlapped crossing tunnels with oblique angles based on the Shanghai Railway transportation project and in situ monitoring data. Hu et al. [13] discussed in detail the criteria and measures for controlling the soil and tunnel deformation. Sharma et al. [14] found that the stiffness of the tunnel lining has significant influence on the displacement and distortion of tunnels caused by an adjacent excavation. In works [15, 16], different numerical simulation methods were also used to evaluate the influence zone of the adjacent construction. In theoretical deduction, the influence zone of the adjacent construction was often simplified to the elastic mechanics analysis and calculation of double-hole or multihole tunnel excavation. Classical solutions are as follows: Peck formation loss model [17], Sagaseta "mirror method" [18], and Howland [19] infinite circular hole stress function. Ng et al. [20] designed and carried out two three-dimensional centrifuge tests in dry sand to investigate the effects of a basement excavation on an existing tunnel located in two horizontal offsets in relation to the basement. Zhao et al. [21] determined the additional stress of shield tunneling on the basis of Mindlin solution of elastic mechanics to evaluate the influence range. Zhang et al. [22] used a viscoelastoplastic model (VEP model) to simulate the rheologic deformation of soil and studied the behavior of the tunnel underneath excavation by the new method to discuss the influence of different factors, including excavation area, relative distance, and construction procedure. Nawel et al. [23] used Finite Element Method to simulate numerically the interaction effects caused by construction of two parallels tunnels. Wei et al. [24] presented a method for security discrimination of adjacent underground pipelines during the construction of twin shield tunnel. Ding et al. [25] analyzed the law of soil displacement caused by shield tunnel construction of adjacent buildings. Liang et al. [26] proposed a simplified analytical method to predict the shield tunnel behaviors associated with adjacent excavation by introducing the Pasternak foundation model with a modified subgrade modulus. Asano et al. [27] presented an observational excavation control method for a mountain tunnel excavated adjacent to an existing tunnel in active service. Xu et al. [28] obtained the stress expressions of mutual influence of parallel tunnels from the point of view of linear elasticity and proposed the concept of interference coefficient in the proximity construction impact zoning.

Summarizing previous studies, it is found that the current research on the influence zone of tunnel adjacent construction is rarely about the underwater tunnel. Using the Japanese tunnel construction guidelines as examples, all of them are comprehensively evaluated on the basis of distance, engineering geology, and construction design. When applied to underwater tunnels, it is insufficient due to the lack of consideration of water weakening and permeation to surrounding rock. In addition, most scholars use the Mohr–Coulomb failure criterion for the theoretical analysis. Based on the development of constitutive models of rock mass in recent years, the Hoek–Brown failure criterion is considered as a more universal model. The Hoek–Brown nonlinear theory is extensively used in various kinds of problems due to its relatively accurate solutions. In this study, based on the Hoek-Brown yield criterion, considering the influence of water seepage, the elastoplastic analysis of the underwater tunnel construction is carried out, and the method of zoning of the underwater tunnel adjacent construction is further proposed. Corresponding the influence zones with the risk levels in the code, then the appropriate control measures are selected on the basis of the risk level to guide the site construction.

2. Elastoplastic Analysis of Surrounding Rock under Seepage Conditions

2.1. Hoek–Brown Failure Criterion and Basic Assumptions. Based on the Griffith brittle fracture theory, the Hoek–Brown failure criterion believed that the cause of rock failure is the deformation and expansion of the existing cracks, which has no significant relationship with the complete rock body yield strength. It is assumed that the rock mass cracks are irregular and the whole rock is isotropic. After years of research and development, the Hoek–Brown failure criterion has been amended several times. Finally, the relationship between rock parameters m, s, α and GSI is established, and its mathematical expression is as follows:

$$\sigma_1 = \sigma_3 + \sigma_c \left(m_b \frac{\sigma_3}{\sigma_c} + s \right)^{\alpha}. \tag{1}$$

In the formula, σ_1 and σ_3 are the maximum and minimum principal stresses when rock mass is destroyed (the compressive stress is positive), σ_c is the uniaxial compressive strength of complete rock mass, and m, s and α are the dimensionless parameter, which have the following equivalent expressions:

$$m_b = m_i \cdot \exp\left[\frac{(GSI - 100)}{(28 - 14D)} \right]. \tag{2}$$

$$s = \exp\left[\frac{(GSI - 100)}{(9 - 3D)} \right]. \tag{3}$$

$$\alpha = \frac{1}{2} + \frac{\left(e^{-GSI/15} - e^{-20/3}\right)}{6}. \quad (4)$$

In the formula, D is the disturbance factor that reflects the type of rock mass, and GSI reflects the integrity of rock mass.

Based on the revised Hoek–Brown failure criterion, the elastic–plastic stress state of underwater tunnel excavation is analyzed, and the calculation model is shown in Figure 1. In the model, the tunnel section shape is circular, the radius of the tunnel is a, the inner water head is h_a, the surrounding rock plastic zone radius is R_p, the water head at the edge of the plastic zone is h_p, the normal stress at the interface between the elastic zone and the plastic zone is P_p, and the elastic zone radius is R_e, the water head far enough is h_0, the original rock stress of the surrounding rock is P_0, and the lining support force is P_a. In order to simplify the calculation model and the solution process, the following basic assumptions are made during the solution of the circular tunnel: (1) assuming that the surrounding rocks around the tunnel are homogeneous rocks, and ignoring the self–weight of the calculation unit, the lateral pressure coefficient is 1.0; (2) with the same permeability coefficient of rocks, the seepage direction is radial to form a stable seepage field; (3) the tunnel lining support force is evenly distributed along the radial direction; (4) the length of the tunnel is long enough to handle the problem as axially symmetric plane strains during calculation; (5) finally, the elastoplastic analysis of the surrounding rock follows the Hoek–Brown failure criterion.

2.2. Seepage Field Status Calculation. According to Darcy's law and the continuity equation of seepage flow in the underwater tunnel, the seepage continuous equilibrium differential equation (5) can be obtained. Equations (6) and (7) are the seepage flow boundary conditions which are expressed as follows:

$$\frac{\partial^2 H}{\partial r^2} + \frac{1}{r}\frac{\partial H}{\partial r} = 0, \quad (5)$$

$$H(r)_{r=a} = h_a, \quad (6)$$

$$H(r)_{r=R_e} = h_0. \quad (7)$$

Combined with above equations, the water head $H(r)$ can be obtained:

$$H(r) = \frac{1}{\ln(R_e/a)}\left(h_0 \ln\frac{r}{a} + h_a \ln\frac{R_e}{r}\right). \quad (8)$$

2.3. Elastic–Plastic Zone Stress State Calculation. When the stress state of the elastic–plastic zone of the surrounding rock is calculated, the seepage water pressure acts on the unit in the form of volume force, and the expression is as follows:

$$f_r = -\gamma_w \frac{d(\xi H)}{dr} = \frac{\gamma_w \xi (h_a - h_0)}{r \ln k}. \quad (9)$$

Considering the effect of seepage volume force, according to elastoplastic calculation principle, the balance differential equation of elastic zone unit is expressed as follows:

$$\frac{d\sigma_r}{dr} + \frac{\sigma_r - \sigma_\theta}{r} + \frac{\gamma_w \xi (h_a - h_0)}{r \ln k} = 0. \quad (10)$$

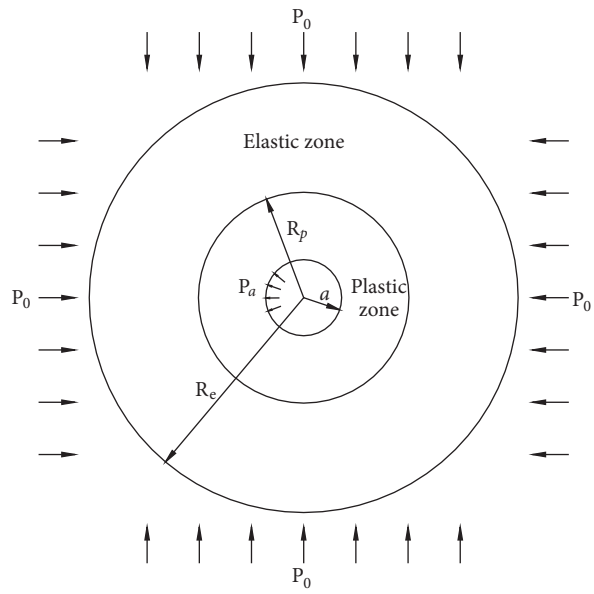

Figure 1: Calculation model of surrounding rock.

In the formula, σ_r is radial stress; σ_θ is tangential stress (tensile stress is positive and compressive stress is negative). γ_w is the weight of water, ξ is the equivalent pore water pressure coefficient, and $k = R_e/a$.

After the unit is deformed, according to the displacement–strain geometric equation (11) and the physical stress–strain physical equation (12), then combined with the equilibrium differential equation, (13) can be obtained:

$$\begin{aligned} \varepsilon_\theta &= \frac{u}{r}, \\ \varepsilon_r &= \frac{du}{dr}, \\ \gamma_{r\theta} &= 0, \end{aligned} \quad (11)$$

$$\begin{aligned} \sigma_r &= \frac{(1-\mu)E}{(1+\mu)(1-2\mu)}\left(\varepsilon_r + \frac{\mu}{1+\mu}\varepsilon_\theta\right) \\ \sigma_\theta &= \frac{(1-\mu)E}{(1+\mu)(1-2\mu)}\left(\varepsilon_\theta + \frac{\mu}{1+\mu}\varepsilon_r\right). \end{aligned} \quad (12)$$

$$\begin{aligned} u = C_3 r + \frac{C_4}{r} + \frac{(1+\mu)(1-2\mu)}{2(1-\mu)E} \\ \times \frac{\xi\gamma_w (h_0 - h_a)}{\ln k} r \ln r. \end{aligned} \quad (13)$$

After introducing the elastic boundary condition equation (14), the expression of stress state in the elastic zone of surrounding rock considering the seepage condition can be solved as (15) and (16):

$$\sigma_r\big|_{r=R_p} = P_p,$$
$$\sigma_r\big|_{r=R_e} = P_0\,. \tag{14}$$

$$\sigma_r = P_0 + \frac{\xi\gamma_w (h_0 - h_a)\ln(r/R_e)}{2(1-\mu)\ln(1/k)} + \frac{{R_p}^2}{{R_p}^2 - {R_e}^2} \times \left(\frac{{R_e}^2}{r^2} - 1\right) \cdot \left[P_0 - P_p + \frac{\xi\gamma_w (h_0 - h_a)\ln\left(R_p/R_e\right)}{2(1-\mu)\ln(1/k)}\right]. \tag{15}$$

$$\sigma_\theta = P_0 + \frac{\xi\gamma_w (h_0 - h_a)\left[\ln(r/R_e) + 2\mu - 1\right]}{2(1-\mu)\ln(1/k)} - \frac{{R_p}^2}{{R_p}^2 - {R_e}^2} \times \left(\frac{{R_e}^2}{r^2} + 1\right) \times \left[P_0 - P_p + \frac{\xi\gamma_w (h_0 - h_a)\ln\left(R_p/R_e\right)}{2(1-\mu)\ln(1/k)}\right]. \tag{16}$$

When the stress state of the plastic zone is calculated, the surrounding rock follows the Hoek–Brown failure criterion in the plastic zone. According to the force analysis when $\lambda = 1$, it can be known the tangential pressure σ_θ is the maximum principal stress σ_1 and the radial stress σ_r is the minimum principal stress σ_3, the Hoek–Brown failure criterion is expressed as follows:

$$\sigma_\theta = \sigma_r + \sigma_c\left(m_b\frac{\sigma_r}{\sigma_c} + s\right)^\alpha. \tag{17}$$

The equilibrium equation of the unit can be changed into (18) as follows:

$$\frac{d\sigma_r}{dr} - \frac{\sigma_c\left(m_b(\sigma_r/\sigma_c) + s\right)^\alpha}{r} + \frac{\gamma_w\xi(h_0 - h_a)}{r\ln k} = 0. \tag{18}$$

After integrating (18), (19) and (20) can be obtained. According to (20), the amount of change of the radial stress along the radial direction in the plastic zone can be determined. Furthermore, according to (17), the amount of change of the tangential stress along the radial direction in the plastic zone can be determined:

$$\int_{P_a}^{\sigma_r} \frac{d\sigma_r}{\sigma_c\left(m_b(\sigma_r/\sigma_c) + s\right)^\alpha - \gamma_w\xi(h_0 - h_a)/\ln k} = \int_a^r \frac{dr}{r} = \ln\frac{r}{a}. \tag{19}$$

$$r = a \times \exp\left[\int_{P_a}^{\sigma_r} \frac{d\sigma_r}{\sigma_c\left(m_b(\sigma_r/\sigma_c) + s\right)^\alpha - \gamma_w\xi(h_0 - h_a)/\ln k}\right]. \tag{20}$$

2.4. Calculation of the Radius of Loose Zone–Bearing Zone. According to the definition of the "loose area", it is assumed that the tangential stress on the boundary of the loose area is the original rock stress, that is $\sigma_\theta = \sigma_p$, then it can be obtained according to the Hoek-Brown failure criterion:

$$\sigma_\theta = \sigma_l + \sigma_c\left(m_b\frac{\sigma_l}{\sigma_c} + s\right)^\alpha = P_0. \tag{21}$$

Substituting (21) into (20), the radius of the loose zone can be obtained as follows:

$$R_L = a\cdot\exp\left[\int_{P_a}^{\sigma_l} \frac{d\sigma_r}{P_0 - \sigma_r - \gamma_w\xi(h_0 - h_a)/\ln k}\right] = \frac{a\left[P_0 - P_a - \gamma_w\xi(h_0 - h_a)/\ln k\right]}{\left[P_0 - \sigma_l - \gamma_w\xi(h_0 - h_a)/\ln k\right]}. \tag{22}$$

It can be seen from (22) that the mechanical parameters of rock mass, groundwater pressure, and seepage effect have a great influence on the radius of the loose zone. Meanwhile, the larger the section size of the excavation tunnel, the larger the radius, whereas the larger the tunnel support force P_a, the smaller the radius.

The radius of the bearing zone can be determined by the following:

$$\int_{R_p}^{R_{b0}} (\sigma_{\theta e} - P_0)\,dr = \frac{1}{2}\int_{R_p}^{R_e} (\sigma_{\theta e} - P_0)\,dr. \tag{23}$$

By substituting (12) into (23), the radius of the bearing zone R_{b0} can be obtained.

$$\int_{R_p}^{R_{b0}} \left[\frac{\xi\gamma_w (h_0 - h_a)\left[\ln(r/R_e) + 2\mu - 1\right]}{2(1-\mu)\ln(1/k)} + \frac{{R_p}^2}{{R_p}^2 - {R_e}^2} \times \left(\frac{{R_e}^2}{r^2} + 1\right) \times \left[P_0 - P_p + \frac{\xi\gamma_w (h_0 - h_a)\ln\left(R_p/R_e\right)}{2(1-\mu)\ln(1/k)}\right]\right] = \frac{1}{2} \cdot \int_{R_p}^{R_e} \left[\frac{\xi\gamma_w (h_0 - h_a)\left[\ln(r/R_e) + 2\mu - 1\right]}{2(1-\mu)\ln(1/k)} + \frac{{R_p}^2}{{R_p}^2 - {R_e}^2} \times \left(\frac{{R_e}^2}{r^2} + 1\right) \times \left[P_0 - P_p + \frac{\xi\gamma_w (h_0 - h_a)\ln\left(R_p/R_e\right)}{2(1-\mu)\ln(1/k)}\right]\right]. \tag{24}$$

3. Underwater Tunnel Adjacent Construction Influence Zones Division

After the excavation of the underwater tunnel, the initial stress equilibrium state of the surrounding rock is damaged and the stress is redistributed. The rock stress around the tunnel exceeds the yield stress of the rock mass and the rock

becomes damaged or enters the plastic state. Subsequently, the stress of the plastic zone around the tunnel is partly transferred to the deep rock mass due to the stress redistribution, while the other part is relieved and eliminated due to the deformation. As the distance from the cave wall increases, the minimum radial principal stress increases and the bearing capacity of the rock mass also increases, which makes the stress state of the surrounding rock transition from plastic state to elastic state in space.

Compared with the initial state of stress, the plastic zone of surrounding rock can be divided into the bearing zone and the loose zone after excavation. The area in the deep plastic zone where the stress is higher than the initial stress and the area with the higher stress in the elastic area of the surrounding rock are combined as the "bearing zone", while the area whose stress is lower than the initial stress is the "loose zone". In the loose zone, the stress and crack propagation of the surrounding rock increase, and the plastic slip is obvious. When the surrounding rock reaches the plastic state, all mechanical parameters are deteriorated. At the same time, the "weak" surrounding rock structure is further weakened by the action of groundwater through pore hydrostatic pressure and hydrodynamic pressure, which makes it easier to damage.

According to the above analysis of the stress state of the surrounding rock after the underwater tunnel excavation and the stress graph of the surrounding rock, the influence zone of the adjacent construction is divided. The loose and bearing zones are considered to be the strong influence zone. In the elastic zone, under the elastic stress state, the range of tangential stress at the hole edge greater than or equal to 1.01 times of the initial stress is defined as the elastic stress concentration zone. Therefore, the stress concentration zone in the elastic zone can be regarded as the weak influence zone and the outer zone is an initial stress zone. The influence zones division is shown in Figure 2.

Based on the Hoek-Brown failure criterion, the loose zone can be divided into three regions, the strong influence, weak influence, and no influence zones, and the strong influence zone can be divided into extensively strong influence, strong influence, and fairly strong influence zones.

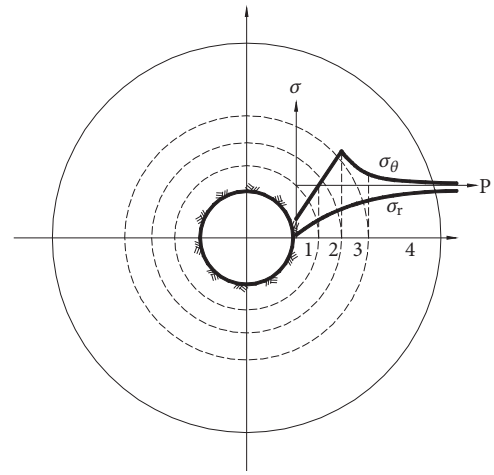

Figure 2: Elastic–plastic stress status of the surrounding rock in underwater tunnel. In the figure, 1 and 2 are the plastic, and 3 and 4 are the elastic zones; 1 is the loose zone, 2 and 3 are the bearing zones, and 4 is the elastic stress concentration zone.

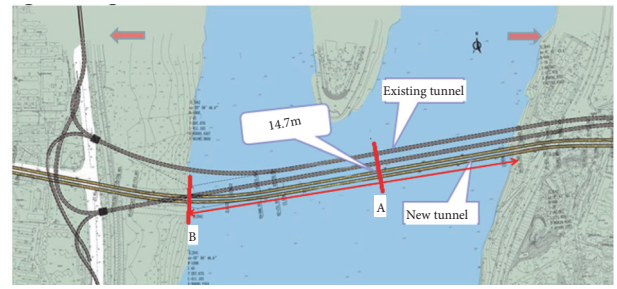

Figure 3: Location of the engineering example.

4. Engineering Example

The research on the influence zone division of the adjacent construction has a strong guiding role in the design and construction of underwater tunnels. For example, when the adjacent construction is in a strong influence zone, reinforcement and support are required. When it is in a weak influence zone, monitoring measures are needed. When it is in a no influence zone, no measures are needed. Figure 3 is an example of underwater shield tunnel engineering.

The underwater tunnel adopts Φ6250 earth pressure balance shield machine construction. Under the river, the left tunnel is parallel to the existing tunnel main line; the minimum spacing between the outer contour of the tunnel and the outer contour of the existing tunnel is 14.700m. Then below the river bank, new tunnel underpasses the existing tunnel; the vertical distance from the outer contour of the new tunnel to the main floor of the existing tunnel is 5.442 m. The riverbed strata are mainly highly weathered conglomerate, and moderately weathered conglomerate exists locally. Two typical sections are selected for calculation and analysis. According to geological data, the water depth of the river in section A is 6 m, the depth of the shield tunnel is 10.906 m, and the whole tunnel is in strong weathered conglomerate. The water depth of river in section B is 1 m, the depth of the shield tunnel is 26.73 m, and the tunnel is also in strong weathered conglomerate.

The relevant parameters at section A are as follows: the tunnel radius is a = 3.14 m, the inner water head is h_a = 0 m, the water head far enough is h_0 = 20 m, the original rock stress of surrounding rock is P_0 = 0.4 MPa, the equivalent pore water pressure coefficient is ξ = 1.0, the surrounding rock elastic modulus is E = 45 MPa, Poisson's ratio is μ = 0.3, the cohesion is c = 50 kPa, and the internal friction angle is φ = 37°.

By substituting r = R_p in Equation (19), the radial stress P_p of the surrounding rock at the elastic–plastic zone can be obtained. Then the plastic zone radius R_e can be obtained. Combined with the relevant parameters of surrounding rock and tunnel, the radius of the plastic zone after the excavation of tunnel is 5.76m.

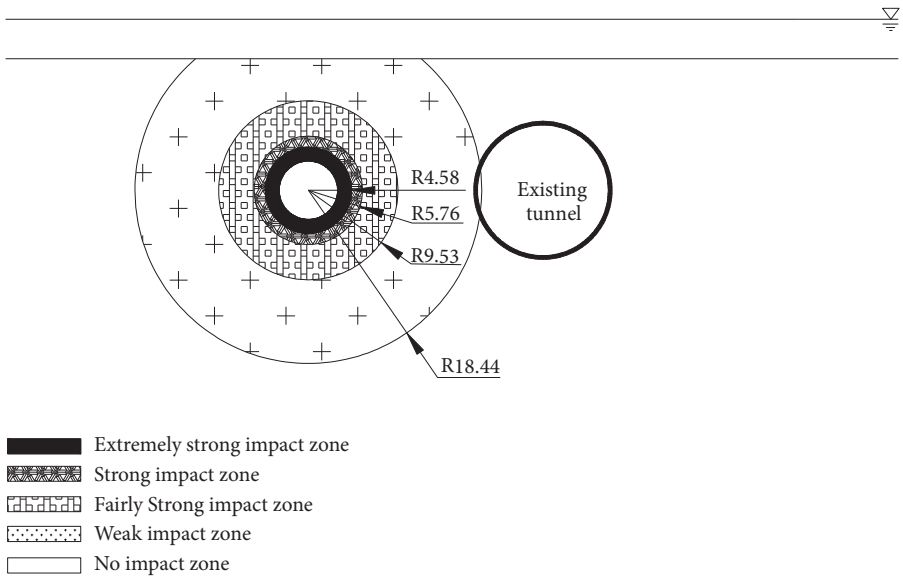

Figure 4: Influence zones of section A.

The radii of the loose zone and the bearing zone are further solved according to (22). When substituting the surrounding rock and tunnel parameters into the equation, the following can be obtained: the loose and bearing zones radii are 4.58 m and 9.53 m. Therefore, the range of extensively strong influence zone is 3–4.58 m, the range of strong influence zone is 4.58–5.76 m, and the range of fairly strong influence zone is 5.76–9.53 m. After solving the radius of the loose and bearing zones, according to (15) and (16), then combining the calculation result of the plastic zone, the following can be obtained: the radius of stress concentration in the elastic zone is 18.44 m, so the radius of the weak influence zone is 18.44 m. The influence zones of section A are shown in Figure 4.

The relevant parameters at section B are as follows: the tunnel radius is a = 3.14 m, the inner water head is h_a = 0 m, the water head far enough is h_0 = 10 m, the original rock stress of surrounding rock is P_0 = 0.5 MPa, and the equivalent pore water pressure coefficient is ξ = 1.0; and the surrounding rock elastic modulus is E = 50 MPa, the Poisson's ratio is μ = 0.2, the cohesion is c = 55 kPa, and the internal friction angle is φ = 40°.

Based on the process of calculating the radius of the influence zones in section A, the radius of the influence zones in section B can be calculated as follows.

It can be obtained from (19) that the radius of the tunnel excavation plasticity influence zone is 6.17m, then the radius of the loose zone is 4.72m and the radius of the bearing zone is 8.28m. Therefore, the range of extensively strong influence zone is 3–4.72 m, the range of strong influence zone is 4.72–6.17 m, and the range of fairly strong influence zone is 6.17–8.28 m. Similarly, the radius of the stress concentration zone in the elastic zone is 15.22m, so the radius of the weak influence zone is 15.22m.The influence zones of section B are shown in Figure 5.

5. Adjacent Construction Influence Zones and Risk Classification

On the basis of the adjacent construction influence zone division, different influence zones of the adjacent construction are associated with different risk levels in the risk assessment, so that the risk level can be determined according to different influence zones during construction. Then the corresponding measures can be taken. Different countermeasures are adopted for the adjacent construction with different risk levels, which has guiding significance for the actual project.

Referring to ≪GB50652–2011 underground rail transit urban construction risk management practices≫ [29], ≪GB / T 50839–2013 urban rail transit safety control technical specifications≫ [30], and ≪CJJ / T 202–2013 urban rail transit structural safety protection technical specifications≫ [31], the influence zones obtained above and risk levels are corresponded. Different risk levels should be taken different risk disposal guidelines and control plans, as shown in Table 1.

6. Control Measures

For the adjacent construction, three aspects can be controlled: one is to reinforce the existing structure, the other is to strengthen the new structure, and the third is to take measures against the soil between the existing and the new structures. Therefore, the following measures can be taken for the adjacent construction.

(1) Measures to be taken for the existing tunnels or projects: the types of countermeasures include basic measures, strengthening measures, and repairing measures. The basic measures include backfilling grouting and prevent tunnel lining off the block. Strengthening measures include the use of arches, anchorage, and crossbar to strengthen

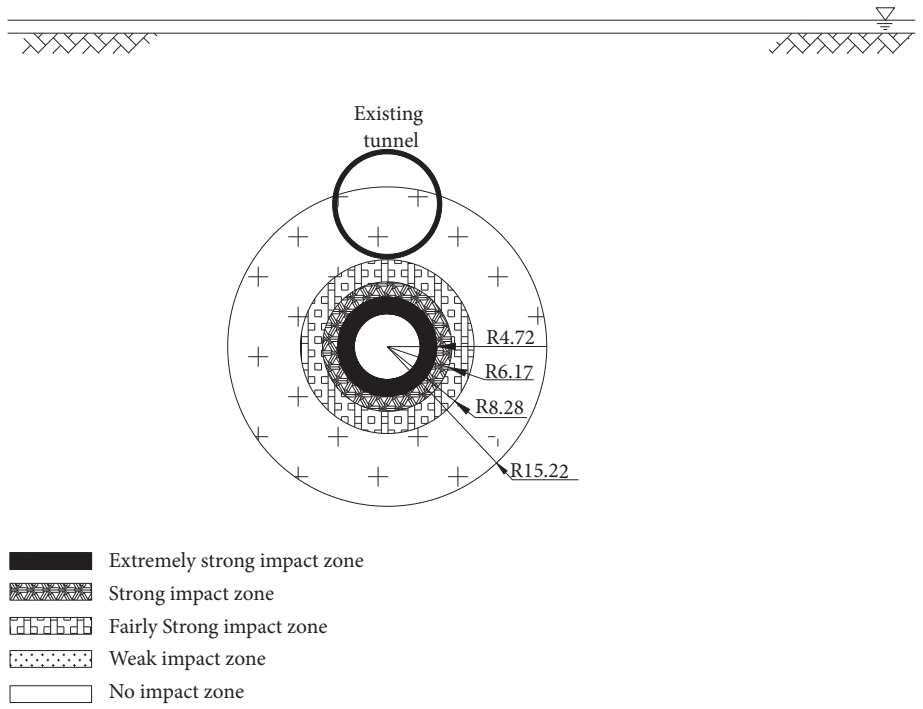

Figure 5: Influence zones of section B.

tunnel linings. Repairing measures include stripping of floating blocks that may fall off, cleaning the surface of the tunnel lining, repairing drainage ditch, and preventing water leakage.

(2) Measures to be taken for the new tunnels or projects: when construction has to be conducted in a strong-influence zone, in order to reduce the impact on the existing tunnel, a more perfect construction scheme or new countermeasures should be developed. The concrete measures include adjusting the driving parameters and changing the supporting structure of lining.

(3) Measures to be taken for the surrounding rock between the existing and the new construction or projects: when the adjacent construction has a bad influence, the protection of the existing tunnel and the measures taken to the side of the new construction are insufficient; measures should be taken to deal with the intermediate strata in order to reduce or eliminate the impact. Generally, methods such as grouting method and freezing method are adopted to strengthen and improve the stratum, and methods of isolating influence may also be adopted, such as underground continuous walls, pipe sheds, steel pipe piles, and arch protection.

Under normal circumstances, the above measures are not completely independently used, and comprehensive application can achieve better control effect. In addition, construction monitoring is an important part of underground engineering. Due to the high risk, complexity, and unpredictability of adjacent construction, monitoring is even more significant. Monitoring data must be fed back in time to guide follow-up construction.

Based on the influence degree of the adjacent construction, the risk level is judged, and then the actual situation of the site is combined to take corresponding measures. For the grade I risk level, the existing structure, the new structure, and the surrounding rock between the existing structure and the new structure should be taken reinforcement measures. For the grade II risk level, the new structure and the surrounding rock between the existing structure and the new structure should take reinforcement measures, and the monitoring of existing structures is needed. For the grade III risk level, the surrounding rock between the existing structure and the new structure should take reinforcement measures, and the monitoring of the existing and the new structures are needed. For the grade IV risk level, the monitoring of the existing and the new structures are needed so as to grasp the impact of construction in real time.

7. Conclusions

In this paper, based on the Hoek–Brown failure criterion, the theoretical analysis is conducted on the underwater tunnel adjacent construction. In consideration of seepage flow, the influence zone of underwater tunnel adjacent construction is divided, then influence zones are matched with risk levels in the code. The following conclusions can be obtained.

(1) The elastic–plastic stress state of the surrounding rock of underwater tunnel is different from that of ordinary tunnel. The seepage action can cause a certain degree of deterioration to the surrounding rock, which cannot be ignored.

(2) According to the proposed zoning method for the influence zone of underwater tunnel adjacent construction in

Table 1: Adjacent construction influence zone and risk classification.

No.	Adjacent construction influence zone	Risk level	Accepted guidelines	Disposal guidelines	Control plans
1	Extensively influence zone	Level I	Unacceptable	Risk control measures must be implemented to reduce the risk, at least to a level that is either acceptable or unwilling	Risk warning and emergency response programs, or program amendments or adjustments should be prepared
2	Strong influence zone	Level II	Unwilling to accept	Risk management should be implemented to reduce risk, and the cost of risk reduction should not be higher than the risk after the risk of loss	Risk prevention and monitoring should be implemented and risk management measures should be formulated
3	Fairly Strong influence zone	Level III	Acceptable	Risk management should be implemented and risk management measures can be taken	The daily management and monitoring frequency should be increased
4	Weak influence zone	Level IV	Ignorable	Can implement risk management	Examination can be conducted daily
5	No influence zone	None	No	No need to consider the risk	General management should be checked

this study, the influence zone can be divided into extensively strong, strong, fairly strong, weak, and no-impact zones. During the construction, measures will be taken on the basis of the different influence zone.

(3) The influence zones are matched with the risk levels, and different countermeasures are taken according to different risk levels, which have guiding significance for the site construction.

Symbols

σ_1: The maximum principal stress, MPa
σ_3: The minimum principal stress, MPa
σ_c: The uniaxial compressive strength of complete rock mass, MPa
m: The dimensionless parameter
S: The dimensionless parameter
α: The dimensionless parameter
D: The disturbance factor that reflects the type of rock mass
GSI: The integrity of rock mass
a: The radius of the tunnel, m
h_a: The inner water head, m
R_p: The surrounding rock plastic zone radius, m
h_p: The plastic zone radius head, m
P_p: The elastic–plastic contact interface at the normal stress, N
R_e: The elastic zone radius, m
R_L: The loose zone radius, m
h_0: The water head far enough, m
P_0: The original rock stress of the surrounding rock, N
P_a: The lining support force, N
σ_r: The radial stress, MPa
σ_θ: The tangential stress, MPa
γ_w: The unit weight of water
ξ: The equivalent pore water pressure coefficient.

Data Availability

The data used to support the findings of this study are available from the corresponding author upon request.

Additional Points

Outlook. Some issues remain to be addressed in future studies. In the latter study, field test and model experiments will be carried out to improve the calculation method of the adjacent construction influence zone division. Further a construction manual to guide the adjacent-construction will be prepared, and a complete set of adjacent-construction technology will be formed to ensure the safety of construction.

Conflicts of Interest

The authors declare that there are no conflicts of interest regarding the publication of this study.

Acknowledgments

The study presented in this article is supported by the National Science Foundation of China, Research Grant no. 50908234.

References

[1] Design Manual, *Tunnel Construction, Maintenance Edition (Adjacent Construction)*, Japan Highway Public Corporation, 1998.

[2] W. G. Chou, *The study on mechanics principle and countermeasure of approaching excavation in underground works [Ph.D. Dissertation]*, Southwest Jiao tong University, Chengdu, China, 2003.

[3] J. L. Du, *In-Situ Experimental Research on Soil Disturbance Characteristics during The Shield Construction Process When Large Shield Was Crossing Existing Subway*, Shanghai Jiao Tong University, Shanghai, China, 2009.

[4] C.-L. Li and L.-C. Miao, "Determination of the range of shield tunneling-induced soil disturbance," *Yantu Lixue/Rock and Soil Mechanics*, vol. 37, no. 3, pp. 759–766, 2016.

[5] X. Huang, H. Huang, and D. Zhang, "Centrifuge modelling of deep excavation over existing tunnels," *Proceedings of the Institution of Civil Engineers: Geotechnical Engineering*, vol. 167, no. 1, pp. 3–18, 2014.

[6] Y. F. Xu, J. S. Chen, and D. M. Fu, "Effect of shield tunneling on mechanical properties of soils," *Chinese Journal of Rock Mechanics and Engineering*, vol. 22, no. 7, pp. 1174–1179, 2003 (Chinese).

[7] C. F. Tao and Y. Chen, "Calculation and analysis of plastic area and ground settlement for shield tunnel," *Modern Transportation Technology*, vol. 6, no. 5, pp. 55–57, 2009.

[8] X. Huang, H. F. Schweiger, and H. Huang, "Influence of deep excavations on nearby existing tunnels," *International Journal of Geomechanics*, vol. 13, no. 2, pp. 170–180, 2013.

[9] M.-N. Wang, X.-J. Zhang, M.-Z. Gou, and G.-Y. Cui, "Method of three-dimensional simulation for shield tunneling process and study of adjacent partition of overlapped segment," *Yantu Lixue/Rock and Soil Mechanics*, vol. 33, no. 1, pp. 273–279, 2012.

[10] B. Liu, D. Zhang, and L. Fang, "Structural response of existed metro tunnels to adjacent large-section pipe jacking construction," *Procedia Engineering*, vol. 189, pp. 11–17, 2017.

[11] V. Avgerinos, D. M. Potts, and J. R. Standing, "Numerical investigation of the effects of tunnelling on existing tunnels," *Tunnelling in the Urban Environment*, vol. 67, no. 9, pp. 808–822, 2018.

[12] Z. Zhang and M. Huang, "Geotechnical influence on existing subway tunnels induced by multiline tunneling in Shanghai soft soil," *Computers & Geosciences*, vol. 56, pp. 121–132, 2014.

[13] Z. F. Hu, Z. Q. Yue, J. Zhou, and L. G. Tham, "Design and construction of a deep excavation in soft soils adjacent to the Shanghai Metro tunnels," *Canadian Geotechnical Journal*, vol. 40, no. 5, pp. 933–948, 2003.

[14] J. S. Sharma, A. M. Hefny, J. Zhao, and C. W. Chan, "Effect of large excavation on deformation of adjacent MRT tunnels," *Tunnelling and Underground Space Technology*, vol. 16, no. 2, pp. 93–98, 2001.

[15] M. Fang and Z. Liu, "3D numerical simulation of influence of undercrossing shield construction on existing tunnel," *Journal of Railway Science and Engineering*, vol. 8, no. 1, pp. 67–72, 2011.

[16] J. X. Wang, X. Z. Yang, and B. Ruan, "Numerical simulation of shield tunnel construction on the impact of neighboring piles foundation," *Journal of Railway Science and Engineering*, vol. 11, no. 1, pp. 73–78, 2014.

[17] R. B. Peck, "Deep excavation and tunneling in soft ground. State of the Art Report," in *Proceedings of the 7th International Conference on Soil Mechanics and Foundation Engineering*, vol. 7, pp. 225–290, 1969.

[18] C. Sagaseta, "Analysis of undrained soil deformation due to ground loss," *Géotechnique*, vol. 37, no. 3, pp. 301–320, 1987.

[19] R. C. J. Howland, "Stresses in a plate containing an infinite row of holes," *Proceedings of the Royal Society of London. Series A - Mathematical and Physical Sciences*, vol. 148, no. 864, pp. 471–491, 1935.

[20] C. W. W. Ng, J. Shi, and Y. Hong, "Three-dimensional centrifuge modelling of basement excavation effects on an existing tunnel in dry sand," *Canadian Geotechnical Journal*, vol. 50, no. 8, pp. 874–888, 2013.

[21] Y.-B. Zhao and Z.-M. Zhang, "Additional stress of surrounding soil caused by propelling of shield tunneling," *Yantu Gongcheng Xuebao/Chinese Journal of Geotechnical Engineering*, vol. 32, no. 9, pp. 1386–1391, 2010.

[22] J.-F. Zhang, J.-J. Chen, J.-H. Wang, and Y.-F. Zhu, "Prediction of tunnel displacement induced by adjacent excavation in soft soil," *Tunnelling and Underground Space Technology*, vol. 36, pp. 24–33, 2013.

[23] B. Nawel and M. Salah, "Numerical modeling of two parallel tunnels interaction using three-dimensional finite elements method," *Geomechanics and Engineering*, vol. 9, no. 6, pp. 775–791, 2015.

[24] G. Wei, X. Lin, and R. Jin, "Security discrimination of adjacent underground pipelines during the construction of twin shield tunnels," *Rock and soil Mechanics*, vol. 1, pp. 181–190, 2018.

[25] Z. Ding, X.-J. Wei, and G. Wei, "Prediction methods on tunnel-excavation induced surface settlement around adjacent building," *Geomechanics and Engineering*, vol. 12, no. 2, pp. 185–195, 2017.

[26] R. Liang, W. Wu, F. Yu, G. Jiang, and J. Liu, "Simplified method for evaluating shield tunnel deformation due to adjacent excavation," *Tunnelling and Underground Space Technology*, vol. 71, pp. 94–105, 2018.

[27] T. Asano, M. Ishihara, Y. Kiyota, H. Kurosawa, and S. Ebisu, "An observational excavation control method for adjacent mountain tunnels," *Tunnelling and Underground Space Technology*, vol. 18, no. 2-3, pp. 291–301, 2003.

[28] R. D. Xu and L. S. Xu, "Linear elastic analysis of stress in surrounding rock of double tunnels," *Geotechnical Engineering Technique*, vol. 19, no. 3, pp. 127–129, 2005.

[29] GB 50652, "Code for risk management of underground works in urban rail transit, China," 2011.

[30] GB/T 50839, "Technical code of urban rail transit engineering safety control, China," 2013.

[31] CJJ/T, "Urban rail transit structural safety protection technical specifications, China," 2013.